View metadata, citation and similar papers at core.ac.uk
brought to you by CORE
provided by Brunel University Research Archive

Abdallah, S., Fan, M., Cashell, K.A. Bond-slip behaviour of steel fibres embedded in concrete after exposure to elevated temperatures. Construction & Building Materials, 2017; 140: 542-551.
http://www.sciencedirect.com/science/article/pii/S0950061817303495

Bond-slip behaviour of steel fibres in concrete after exposure to elevated temperatures

Sadoon Abdallah, Mizi Fan* and K.A. Cashell

College of Engineering, Design and Physical Sciences, Brunel University
Uxbridge, UB8 3PH, London, United Kingdom

Abstract

The bond-slip mechanisms, associated with the pull-out behaviour of steel fibres embedded in concrete after exposure to elevated temperatures, are experimentally investigated. A series of pull-out tests have been performed on straight and hooked-end steel fibres embedded in four different types of concrete, namely, normal strength concrete (NSC), medium strength concrete (MSC), high strength concrete (HSC) and ultra-high performance mortar (UHPM). Ninety days after casting, the specimens were heated to a target temperature of either 100, 200, 300, 400, 500, 600, 700 or 800°C. The effect of temperature on the mechanical and thermal properties of the steel fibres and concrete was also studied. The results showed that the bond behaviour of straight fibres is significantly influenced by heating. The influence of elevated temperatures on the bond characteristic of hooked-end fibre was twofold: the bond strength does not vary significantly for all matrixes in 20-400°C, while the bond dramatically degraded in 400-800°C, especially at temperatures greater than 600°C. The reduction in bond strength at elevated temperatures is found to be strongly related to the degradation in properties of the constituent materials, i.e. the fibres and concrete.

Key words:
Bond-slip behaviour; Bond strength; Elevated temperature; Hooked-end fibres; Straight fibres.

**Corresponding author: Professor, Head of Civil Engineering Department and Research Director, Brunel University, Email: mizi.fan@brunel.ac.uk, Tel.: +44 189 5266466*

1. Introduction

Steel fibre reinforced concrete (SFRC) is increasingly common in structural engineering owing to its ease of construction, structural performance and efficiency. Steel fibres are incorporated into cementitious materials in order to improve their ductility and energy absorption, and to resist or delay the development of cracks [1,2]. The main contribution of the fibres is to enable the concrete element to continue carrying loads after cracking has occurred, the so-called post-cracking behaviour [3]. SFRC is vulnerable to severe environmental conditions such as those which occur during a fire. At a high temperature, the mechanical and physical properties of the concrete and reinforcing steel fibres, as well as the bond characteristic between these materials, may significantly deteriorate. Hence, the strength of SFRC under various elevated temperatures can vary, depending mainly on the fibre-matrix bond strength. Therefore, the bond characteristic between the steel fibre and surrounding concrete subject to high temperatures urgently needs to be understood and quantified, especially for hooked-end fibres, which are amongst the most widely used of the various fibres available on the market.

There are two main mechanisms through which bonds develop between the concrete and fibres, namely physiochemical bond (i.e. adhesion and friction) and mechanical bond (i.e. interlock) [4]. The former is predominantly determined by the properties of the interfacial transition zone (ITZ) as well as the fibre surface properties [5]. This type of bond is the first mechanism to be activated in the pull-out process and mainly controls the pull-out resistance of straight fibres. For very plain fibres, with no deformities or bends, this is the only bond mechanism that is present. The second type of bond, mechanical interlock, is determined by the geometric deformations due to the fibre straightening with increasing tensile stress.

Numerous investigations have been conducted to improve the understanding of the bond-slip characteristics between steel fibres and concrete. The most effective mechanism for developing bond strength is through the presence of mechanical deformations in the fibre [6-8]. Whereas the bond characteristics between steel fibres and concrete at ambient temperature have been the subject of intensive investigation by researchers [9-11], for the high-temperature behaviour, information is much more limited, particularly in terms of experimental data. Much of the current knowledge of the high-temperature behaviour of SFRC is based on thermal and mechanical properties tests [12,13].

The behaviour of structural elements and materials in fire conditions is of paramount importance and carefully considered in structural design, particularly for high-rise buildings and other infrastructure. In these construction forms, SFRC is regularly used as a primary structural material [14-17]. The main concern from the structural performance point of view is the condition and integrity of the constituent materials (i.e. steel fibre and concrete) and also the bond characteristics between them, as the temperature increases. It is well established that concrete undergoes significant change in its chemical composition, physical structure and water content when subjected to elevated temperature [18,19]. These physical and chemical changes cause the aggregate to expand, whilst the surrounding cement paste experiences shrinkage. As a result of these transformations, the cement paste-aggregate bond is the weakest point in the concrete mix in fire [20,21]. This thermal mismatch between the aggregate and the cement paste cause the concrete to crack [22]. An assessment of the degree of deterioration in physical and mechanical properties of SFRC after exposure to high temperatures can be achieved by investigating the bond-slip characteristics. The fibre-matrix bond properties are commonly assessed using the single-fibre pull-out test [23].

This paper presents a series of experimental pull-out tests on both straight and hooked-end steel fibres; A total of four groups of concrete mixtures were investigated, which had an initial compressive concrete strength ranging between 33 and 148 MPa. The main objective of this research was to experimentally investigate the bond-slip mechanisms of both straight and hooked-end fibres at ambient and elevated temperature. The results of this experimental investigation are essential to better understand the effects that elevated temperature have on the bond-slip characteristics, and further to predict the post fire-resistance of SFRC structural elements.

2. Experimental programme

2.1. Materials

Four different concrete grades were investigated in these experiments, namely normal strength concrete (NSC), medium strength concrete (MSC), high strength concrete (HSC) and ultra-high performance mortar (UHPM). All were prepared using two classes of Ordinary Portland Cement (i.e. CEM II 32.5R and CEM III 52.5N) according to European standard EN 197-1 [24]. Silica fume, ground quartz and fly ash were also used for the preparation of the MSC, HSC and UHPM mixtures. The aggregates consisted of crushed granite with a maximum size of 10 mm. Coarse sand (0-4 mm) was used in the NSC, MSC and HSC mix

design and very fine sand (150-600 μm) was used in the UHPM mix design. A superplasticizer called TamCem23SSR was used to enhance the workability of the HSC and UHPM mixtures. The mix proportions are summarised in Table 1.

Both straight and hooked-end steel fibres were used in the pull-out tests. The commercial Dramix hooked-end fibres were 60 mm in length (L_f) and 0.90 mm in diameter (D_f), had an aspect ratio (L_f/D_f) of 65, and had tensile strength of 1150 N/mm^2. The geometrical properties of the hooked end fibres are depicted in Fig. 1 and detailed in Table 2. To study the anchorage effect of the hook, straight fibres were obtained by cutting the end hooks of the hooked fibres to ensure the consistency (see Fig. 1b). The cut fibres were examined to ensure only no deformed fibres were selected for experiments.

2.2. Specimens

The pull-out test specimens prepared were 100 mm cubes for NSC, MSC and HSC and 100 × 50 mm cylinders for the UHPM specimens (this is because of the finer aggregates in this mixture). The steel fibre was carefully embedded in the cement mixes. The fibre embedment length was 30 mm, which is half the length of the fibre used in this investigation. For each concrete mix, three additional 100 mm cubes were prepared in order to determine the compressive strength and mass loss of the mixture for each thermal level. Immediately after casting and vibration, the specimens were covered with a thin polyethylene film in order to minimise moisture loss and left for 24 hours at room temperature. The specimens were demoulded after 24 hours and then cured for a further 28 days in the conditioning chamber, which was controlled to have a temperature of 20 ± 2°C and relative humidity of 95 ± 5%.

2.3. Heating scheme

At 90 days after casting, the specimens for the pull-out and compressive strength tests were placed in an electrical high-temperature furnace. For the pull-out specimens, the free end of the steel fibre was protected with heat insulation before the specimens were placed in the furnace. The specimens were then heated to a maximum target temperature of 100, 200, 300, 400, 500, 600, 700 or 800°C, at a heating rate of 20°C/min [18,25]. The target temperatures were maintained for 1 hour, following which the specimens were allowed to cool down naturally before being tested at room temperature. It is noteworthy that for specimens heated to higher temperatures; the overall exposure duration was greater than for specimens heated to relatively lower temperatures as the specimens also follow the "heating up" period. The

temperature-time curve of the furnace compared with the standard curve recommended in ISO 834[26] and RWS [27] is presented in Fig. 2.

2.4. Test setup

The pull-out tests were performed on the cooled specimens using a specially designed grip system, as illustrated in Fig. 3, which was attached to an Instron 5584 universal testing machine. The grips were designed such that the forces applied to the fibre provided a true reflection of the real situation experienced by fibres bridging a crack. The body of the gripping system was machined in a lathe using mild steel and had a tapered end to allow the insertion of four M4 grub screws (Fig. 3). These were then tightened around the steel fibre to an equal torque to ensure an even distribution of gripping pressure and to minimise deformation or breakage of the fibre ends.

Two linear variable differential transformer transducers (LVDT) were used to measure the distance travelled by the steel fibre relative to the concrete surface during testing (i.e. the pull-out distance). They were held in place using aluminium sleeves on either side of the main grip body (Fig. 3). The LVDT had ball bearings at the tips to allow for accurate readings on the surface of the samples. The sample was secured to the Instron base using clamps with riser blocks and M16 studs. The specimen was positioned on a brass round disc to remove any discrepancies in the sample base and allow for distortion. In all pull-out tests, a displacement rate of 10 μm/s was adopted.

3. Results and discussion

3.1. Effect of elevated temperatures on mechanical and thermal properties of concrete

3.1.1. Compressive strength

The residual compressive strengths (measured as the average of three cubes) of all mixes after exposure to various levels of elevated temperature are plotted in Fig. 4. It is noteworthy that results are only presented for the UHPM mix up to 400°C because explosive spalling occurred at higher temperatures, and the compression strength of concrete at elevated temperature (f'_{cT}) is normalised by the corresponding value at ambient temperature (f'_c). As expected, an exposure to higher temperatures caused a general degradation of all mixes, with the compressive strengths consistently decreasing after any level of elevated temperature exposure, except that at 200°C for NSC, MSC and HSC, which showed a slight increase in compressive strength owing to rehydration and moisture migration, while for the UHPM mix,

the compressive strength continues to increase up to 300°C before dropping at 400°C. It was observed that explosive spalling did not occur for any of the tests up to 400°C, but as previously stated, at higher temperatures spalling did occur for UHPM mix, resulting in unreliable results which are not presented herein.

Following exposure to temperatures beyond 300°C, the rate of compressive strength loss of NSC, MSC and HSC becomes significant up to 500°C and then there is a sharp reduction to 800°C. At 800°C, the residual compressive strength of NSC, MSC and HSC were 33%, 42% and 47% of original values respectively. The sharp reduction in compressive strength at this temperature may be attributed to both physical and chemical transformation that takes place in concrete, resulting in the decomposition of calcium silicate hydrate (C-S-H) gel which leads to the loss of binder property in concrete. Interestingly, the HSC maintained a higher percentage value of residual compressive strength than NSC throughout the temperature (400-800°C) range. This is in agreement with other results reported previously [28].

3.1.2. Mass loss

Fig. 5 illustrates the average mass loss as a percentage of the original ambient value (M_{loss}) for all concrete mixtures after exposure to various elevated temperatures. The mass of each specimen was measured before heating and again after cooling in order to determine the mass loss ratio. It is evident that for all mixtures the moss loss was relatively small (<2%) after exposure to temperatures of 300°C, and then the loss increased significantly following temperatures between 300 and 800°C. It is also interesting to observe that the mass loss of MSC between 200 and 600°C is higher than that of NSC. This inconsistency may be due to the MSC having comparatively less water content and more evaporable water than NSC. When temperature reached 800°C, the mass losses of NSC, MSC and HSC were 11%, 10%, and 8% respectively, which was not as significant as that of compressive strength. This indicates that the initial compressive strength and grade of the concrete does not have a great influence on the mass loss [29]. Similar results have been found also by other researchers [30,31].

3.2. Effect of elevated temperatures on the properties of steel fibres

The stress-strain curves obtained from tensile tests on the steel fibres at ambient and various elevated temperatures are shown in Fig. 6. For each temperature increment, a total of six fibres were tested with the same heating regime as used in the concrete tests. The average

results in terms of mechanical properties are summarized in Table 3. As expected, an exposure to higher temperatures significantly degraded the yield and ultimate strengths of the steel fibres. It can be seen in Fig. 6 that the stress-strain behaviour remained relatively unchanged between 20 and 200°C. Between 300-400°C, although the yield and ultimate strengths of the fibres remained high, the stiffness and overall shape of the stress-strain response changed. At higher temperatures (i.e. exposure of 500°C or higher), the strength values greatly decreased and, moreover, there was a significant change in the shape of the stress-strain response. It is apparent that heating the steel fibre to 600°C or above resulted in a significant increase in the ductility (elongation) of the fibres. When the steel fibre attained a maximum temperature of 800°C, the remaining yield and ultimate strengths were about 15 and 25% of their corresponding value at ambient temperature, respectively.

3.3. Bond behaviour at elevated temperatures between the steel fibres and surrounding concrete

In this section, for each temperature increment, the mean values of maximum pull-out load measured in the tests (P_{max}), the maximum fibre stress ($\sigma_{f,max}$), the average and equivalent bond shear stress (τ_{av} and τ_{eq}, respectively) and the total pull-out work (W_{total}) are discussed. The values for τ_{av} and τ_{eq} are commonly applied as criteria to evaluate the bond behaviour between steel fibre and matrix [4,32] and are determined from Eqs.(1) and (2), respectively:

The average bond strength τ_{av} is defined as the average bond strength based on the maximum pull-out load (P_{max}) and the initial embedment length and is given by [4,32]:

$$\tau_{av} = \frac{P_{max}}{\pi \times d_f \times L_E} \qquad (1)$$

The equivalent bond strength τ_{eq} is defined as the average bond strength based on the total work done during pull-out (W_{total}) and is obtained as [33]

$$\tau_{eq} = \frac{2 \times W_{total}}{\pi \times d_f \times {L_E}^2} \qquad (2)$$

where d_f is the fibre diameter and L_E is the initial embedment length. The total work done during pull-out (W_{total}) is calculated as the area under the pull-out load-slip curve.

3.3.1. Straight fibres

Fig. 7 shows the bond stress-slip curve (measured as the average of five specimens) for a straight steel fibre embedded in all four concrete matrixes at ambient and elevated temperatures. It can be seen that a typical bond-stress curve of a straight fibre is characterized by a rapid increase of bond stress until the maximum value is reached and this is generally followed by a sudden drop as the fibre debonds. At some point, generally around 1-2 mm slip, the bond value stabilises at a residual value. Initially, the bond strength is generated by a combination of adhesion and friction. Once the peak bond has been reached, the adhesion is overcome causing a sudden drop in the bond strength. After this, in the residual bond portion of the response, only frictional forces remain until the fibre completely pulls out of the matrix.

The detailed results from the tests are summarised in Table 4, which includes P_{max}, $\sigma_{f,max}$, τ_{av}, τ_{eq} and W_{total} for each concrete type at the various temperature increments. The expression given in Eq. (1) was used to determine the average bond strength (τ_{av}), and this is presented in Fig. 8, which illustrates how this property is influenced by both temperature and concrete mixture. At room temperature, it is shown that there was an increase of around 10%, 63% and 79% in τ_{av} when the concrete strength was increased from 33 MPa to 52, 71 and 148 MPa, respectively (i.e. from NSC to MSC, HSC and UHPM, respectively). The corresponding increase in the equivalent bond strength values (τ_{eq}) determined using Eq. (2) was 9%, 64% and 73%, respectively. It is most likely that the main reason for the enhanced bond strength with increasing concrete strength is due to the improved matrix packing density around the fibre, which leads to higher frictional bond stresses being generated.

After heating higher than 100°C, the loss of bond strength follows similar trend in all mixes. Fig. 9 presents the variation in average bond strength at elevated temperature ($\tau_{av,T}$) normalised by the corresponding values at ambient temperature (τ_{av}) with increasing temperature. It is evident that all of the concrete matrixes showed decreasing bond strength (τ_{av}) with increasing temperature. The τ_{av} of NSC decreased sharply up to 300°C and then gradually reduced in the temperature range of 400-600°C before stabilizing at temperatures between 600 and 700°C, and finally drops sharply again up to 800°C. The reduction in τ_{av} of MSC was also sharp up to 300°C and then remained almost constant between 500 and 600°C, before decreasing sharply again between 600°C and 800°C. The τ_{av} of the straight fibres embedded in HSC also decreased gradually up to 700°C and more sharply between 700°C

and 800°C. It is notable that the level of loss in strength at the temperature range between 200 and 700°C was significantly lower for HSC than those for NSC and MSC. On the other hand, the loss of τ_{av} in the UHPM matrix is steeper than in MSC and HSC, and almost linear until the occurrence of explosive spalling above 400°C. This sharp reduction in bond strength for the UHPM matrix is attributed to the significant degradation in the physicochemical bond properties due to the low permeability and dense microstructure of this mixture. At 800°C, the τ_{av} (Fig. 9) of NSC, MSC and HSC decreased by 84%, 68% and 81% of their original strength respectively. This sharp reduction in bond strength at 800°C is attributed to the significant degradation of material properties as well as the differential thermal expansion between the two materials. It was reported [29,30] that at 800°C the thermal expansion of concrete increased by 1.3% from zero at ambient temperature while that coefficient for steel increases by 20% [34]. These effects combine to result in greater damage and the development of more cracks around the fibre, and hence the reduction of pull-out resistance. The rate of reduction in bond strength of straight fibre at elevated temperature is found to have a similar trend as that of plain rebar previously reported [25,35,36].

Fig. 10 shows the variation in equivalent bond strength at elevated temperature ($\tau_{eq,T}$) normalised by the corresponding values at ambient temperature (τ_{eq}) with increasing temperature. For all concretes, there was a reduction in equivalent bond strength (τ_{eq}) at 100°C initially and then τ_{eq} regain at 200°C, while the τ_{eq} of UHPM appeared to significantly decrease with temperature. Above 300°C the τ_{eq} loss becomes gradual with increase in temperature for NSC and HSC. The τ_{eq} of NSC, MSC and HSC were significantly diminished, relative to the room temperature values, when pull-out specimens were heated to within the 600-800°C temperature range. At 800°C, the τ_{eq} of NSC, MSC and HSC reduced by 64%, 67% and 83%, respectively, compared with their corresponding values at ambient temperature.

3.3.2. Hooked-end fibres

Fig. 11 shows the bond stress-slip curves (measured as the average of five specimens) for hooked-end fibres embedded in NSC, MSC, HSC and UHPM matrixes following exposure to different levels of elevated temperature between 20 and 800°C. It is observed that the bond stress-slip behaviour of hooked-end fibres is significantly different from that of the straight fibres. This may be due to the different bond mechanisms present. For straight fibres, the bond is generated entirely from chemical adhesion and friction. These are also present in

hooked-end fibres but are supplemented by the additional phenomenon of mechanical interlocking between the concrete and fibre, due to plastic deformation in the fibre hooks. Comparison of the graphs in Fig. 11 with the equivalent responses in Fig. 7 shows that the contribution made by this mechanical interlocking mechanism significantly improves the bond-slip characteristic of the hooked-end fibres embedded in all four matrixes. Not only are the maximum bond values much higher for the hooked-end fibres but also the general shape of the bond stress-slip curve is also different. In contrast to the straight fibre behaviour, the descending branch of the hooked-end fibres demonstrated a second localised peak at a slip of around 2-5 mm, this is due to the activation of the mechanical interlocking bond once the adhesion has been overcome.

The shape of the bond stress-slip curve for the hooked-end fibres embedded in concrete is similar for the NSC, MSC and HSC mixes, even at high temperatures. However, there are some differences in terms of the maximum bond stress and pull-out work values. A significant difference is also observed between Fig. 11(a-c) and Fig. 11(d), which plot the average bond stress for each concrete mix. In the latter, the bond stress for UHPM shows a gradual decline immediately following the attainment of τ_{max}, whereas the other concrete mixes exhibit almost plateau after τ_{max} until the second peak which is followed by a gradual decrease in the bond stress. This difference is attributed to the variation in the level of deformation and straightening of the hook which is higher for UHPM than the other matrixes. It is also important to consider that it was observed during the experiments that the end hook of the fibre at 300°C ruptured internally in the hook region at a slip of around 2.7 mm. This represents $\sigma_{f,max}/\sigma_y$ of around 0.93 (where σ_y is the yield strength of the steel fibre at ambient temperature), which reflects a full activation of the mechanical bond. Nevertheless, as illustrated in Fig. 11d, the fibre continued to transfer the stress until the fibre completely pulled out; the hook at the other end of the fibre remained intact.

The average bond strength (τ_{av}) of hooked-end fibres after exposure to various levels of elevated temperature is presented in Fig. 12, whilst the corresponding equivalent bond strength (τ_{eq}) results are given in Table 5. It is evident that τ_{av} and τ_{eq} for the hooked-end fibres increase significantly with increasing concrete compressive strength. Figs. 13 and 14 illustrate the average and equivalent bond stress normalised by the corresponding ambient value for all mixes with increasing temperature. It can be seen that for the four matrixes, both τ_{av} and τ_{eq} follows a decreasing trend with increasing temperature. However, the decrease

does not begin until around 300°C, corresponding with similar findings for the effect of temperature on the compressive strength of concrete presented in Fig. 4. Interestingly, the behaviour of the HSC concrete differs from the other concretes in that it starts to lose bond strength significantly earlier, from around 100°C. This gradual degradation of bond strength may be attributed to the lower permeability and dense microstructure of HSC, which results in a significant strength loss as compared to NSC and MSC. The τ_{av} and τ_{eq} values for the hooked-end fibres embedded in all four matrixes follow similar trend in the higher temperature range (i.e. 400°C-800°C). At 800°C, the τ_{av} of the NSC, MSC and HSC mixes decreased by around 55%, 63% and 55%, respectively, relative to the corresponding ambient values whilst the equivalent values for τ_{eq} were 55%, 52% and 53%, respectively. Interestingly, as shown in Figs. 13 and 14, at 800°C the loss in bond strength for all concrete mixes is almost identical. Therefore, it is deduced that the compressive strength of concrete does not have a significant influence on bond strength loss at elevated temperatures.

3.4. Evaluation of fibre damage

Following the tests, the damage to the fibres after exposure to elevated temperature and being subjected to pulling out from the concrete was evaluated using a high power optical microscope. It is noteworthy that this assessment was conducted for fibres embedded in all four concrete types, but only the NSC images are presented herein for brevity as the results were very similar irrespective of the matrix mix (Fig. 15).

The morphology of the fibre deformation was analysed and it was shown that the specimens exposed to 400°C and above exhibited significant deterioration to the fibre surface, as compared with the fibres exposed to lower temperatures. The fibres pulled out from specimens heated to 400-800°C had clearly changed colour and also developed a corroded surface. These changes are mainly due to the oxidation process which results in surface damage and this is more pronounced at higher temperatures. This phenomenon has also been observed by other authors [37-40]. The deterioration of bond at high temperatures may be caused by both a degradation of the material properties, differential thermal expansion and also their physical changes. This behaviour is also consistent with that observed by Ezziane et al.[41].

4. Conclusions

The bond behaviour between steel fibre and concrete matrix subject to elevated temperature have been characterised with two types of steel fibres and four different concrete mixes. The following conclusions can be drawn:

1) Temperature had a significant influence on the mechanical and thermal properties of both steel fibres and concrete. At the temperature higher than 400°C, the mechanical properties of both materials decreased with increasing temperature. On the other hand, both the mass loss in the concrete and the ductility of the steel fibres increased.
2) The bond strength degraded significantly with increasing temperature in all matrixes for the straight fibres. At 800°C, the average bond strength of NSC, MSC and HSC decreased by 84%, 68% and 81%, respectively. Similarly, the equivalent bond strength τ_{eq} decreased by 64%, 67% and 83%, respectively.
3) The bond-slip characteristic between the hooked fibre and matrix reflected two different temperature ranges, namely 20-400°C and 400-800°C. The bond behaviour in the former range did not vary significantly for all mixes, while in the latter range, the NSC, MSC and HSC lost most of their original bond strength, especially once they were exposed to temperatures greater than 600°C.
4) The reduction in bond strength of both straight and hooked-end fibres was found to be strongly associated with the degradation in material properties (i.e. the fibre and concrete properties). However, the reduction in material properties appears to have a more significant effect on the bond-slip mechanisms of straight fibres compared with hooked-end fibres.

Acknowledgments

The first author gratefully acknowledges the financial support of the Ministry of Higher Education and Scientific Research of Iraqi Government for this Ph.D. project.

References

[1] Romualdi JP, Ramey M, Sanday SC. Prevention and Control of Cracking by Use of Short Random Fibers. Special Publication 1968;20:179-204.

[2] Abu-Lebdeh T, Hamoush S, Heard W, Zornig B. Effect of matrix strength on pullout behavior of steel fiber reinforced very-high strength concrete composites. Constr Build Mater 2011;25:39-46.

[3] Abdallah S, Fan M, Zhou X, Geyt S. Anchorage Effects of Various Steel Fibre Architectures for Concrete Reinforcement. International Journal of Concrete Structures and Materials 2016:1-11.

[4] Wille K, Naaman AE. Pullout behavior of high-strength steel fibers embedded in ultra-high-performance concrete. ACI Mater J 2012;109.

[5] Cunha VM. Steel fibre reinforced self-compacting concrete (from micromechanics to composite behavior). 2010.

[6] Banthia N. A study of some factors affecting the fiber-matrix bond in steel fiber reinforced concrete. Canadian Journal of Civil Engineering 1990;17:610-20.

[7] Laranjeira de Oliveira F. Design-oriented constitutive model for steel fiber reinforced concrete. : Universitat Politècnica de Catalunya, 2010.

[8] Zīle E, Zīle O. Effect of the fiber geometry on the pullout response of mechanically deformed steel fibers. Cem Concr Res 2013;44:18-24.

[9] Beglarigale A, Yazıcı H. Pull-out behavior of steel fiber embedded in flowable RPC and ordinary mortar. Constr Build Mater 2015;75:255-65.

[10] Isla F, Ruano G, Luccioni B. Analysis of steel fibers pull-out. Experimental study. Constr Build Mater 2015;100:183-93.

[11] Abdallah S, Fan M, Rees DWA. Analysis and modelling of mechanical anchorage of 4D/5D hooked end steel fibres. Mater Des 2016;112:539-52.

[12] Kim J, Lee G, Moon DY. Evaluation of mechanical properties of steel-fibre-reinforced concrete exposed to high temperatures by double-punch test. Constr Build Mater 2015;79:182-91.

[13] Sideris KK, Manita P, Chaniotakis E. Performance of thermally damaged fibre reinforced concretes. Constr Build Mater 2009;23:1232-9.

[14] Chen GM, He YH, Yang H, Chen JF, Guo YC. Compressive behavior of steel fiber reinforced recycled aggregate concrete after exposure to elevated temperatures. Constr Build Mater 2014;71:1-15.

[15] Di Prisco M, Plizzari G, Vandewalle L. Fibre reinforced concrete: new design perspectives. Mater Struct 2009;42:1261-81.

[16] Michels J, Waldmann D, Maas S, Zürbes A. Steel fibers as only reinforcement for flat slab construction–experimental investigation and design. Constr Build Mater 2012;26:145-55.

[17] Michels J, Christen R, Waldmann D. Experimental and numerical investigation on postcracking behavior of steel fiber reinforced concrete. Eng Fract Mech 2013;98:326-49.

[18] Haddad RH, Shannis LG. Post-fire behavior of bond between high strength pozzolanic concrete and reinforcing steel. Constr Build Mater 2004;18:425-35.

[19] Düğenci O, Haktanir T, Altun F. Experimental research for the effect of high temperature on the mechanical properties of steel fiber-reinforced concrete. Constr Build Mater 2015;75:82-8.

[20] Hager I. Behaviour of cement concrete at high temperature. Bulletin of the Polish Academy of Sciences: Technical Sciences 2013;61:145-54.

[21] Morley P, Royles R. The influence of high temperature on the bond in reinforced concrete. Fire Saf J 1980;2:243-55.

[22] Fu Y, Wong Y, Poon C, Tang C, Lin P. Experimental study of micro/macro crack development and stress–strain relations of cement-based composite materials at elevated temperatures. Cem Concr Res 2004;34:789-97.

[23] Lee Y, Kang S, Kim J. Pullout behavior of inclined steel fiber in an ultra-high strength cementitious matrix. Constr Build Mater 2010;24:2030-41.

[24] En B. 197-1 (2000) Cement: composition, specifications and conformity criteria for common cements. British Standards Institution, London 2000.

[25] Bingöl AF, Gül R. Residual bond strength between steel bars and concrete after elevated temperatures. Fire Saf J 2009;44:854-9.

[26] International Organization for Standardization. Fire-resistance Tests: Elements of Building Construction. Specific Requirements for Loadbearing Vertical Separating Elements. : ISO, 2000.

[27] Li YZ, Ingason H. The maximum ceiling gas temperature in a large tunnel fire. Fire Saf J 2012;48:38-48.

[28] Chan YN, Peng GF, Anson M. Residual strength and pore structure of high-strength concrete and normal strength concrete after exposure to high temperatures. Cement and Concrete Composites 1999;21:23-7.

[29] Kodur V. Properties of concrete at elevated temperatures. ISRN Civil Engineering 2014;2014.

[30] Khaliq W. Performance characterization of high performance concretes under fire conditions. , 2012.

[31] Zheng W, Li H, Wang Y. Compressive behaviour of hybrid fiber-reinforced reactive powder concrete after high temperature. Mater Des 2012;41:403-9.

[32] Wille K, Naaman A. Bond stress-slip behavior of steel fibers embedded in ultra high performance concrete. 2010:99-111.

[33] Kim DJ, El-Tawil S, Naaman AE. Loading rate effect on pullout behavior of deformed steel fibers. ACI Mater J 2008;105.

[34] Elghazouli A, Cashell K, Izzuddin B. Experimental evaluation of the mechanical properties of steel reinforcement at elevated temperature. Fire Saf J 2009;44:909-19.

[35] Ergün A, Kürklü G, Başpınar MS. The effects of material properties on bond strength between reinforcing bar and concrete exposed to high temperature. Constr Build Mater 2016;112:691-8.

[36] Xiao J, Hou Y, Huang Z. Beam test on bond behavior between high-grade rebar and high-strength concrete after elevated temperatures. Fire Saf J 2014;69:23-35.

[37] Barburski M, Lomov SV. Influence of oxidation on steel fiber yarn and knitted fabric properties. Journal of Industrial Textiles 2016;45:1516-29.

[38] Ezziane M, Molez L, Jauberthie R, Rangeard D. Heat exposure tests on various types of fibre mortar. European journal of environmental and civil engineering 2011;15:715-26.

[39] Sukontasukkul P, Pomchiengpin W, Songpiriyakij S. Post-crack (or post-peak) flexural response and toughness of fiber reinforced concrete after exposure to high temperature. Constr Build Mater 2010;24:1967-74.

[40] Vesel A, Mozetic M, Drenik A, Hauptman N, Balat-Pichelin M. High temperature oxidation of stainless steel AISI316L in air plasma. Appl Surf Sci 2008;255:1759-65.

[41] Ezziane M, Molez L, Kadri T, Jauberthie R, Gouttefangeas F. Adhérence fibre d'acier–matrice cimentaire dans les mortiers fibrés à hautes températures. 2012:1192.

Abdallah, S., Fan, M., Cashell, K.A. Bond-slip behaviour of steel fibres embedded in concrete after exposure to elevated temperatures. Construction & Building Materials, 2017; 140: 542-551.
http://www.sciencedirect.com/science/article/pii/S0950061817303495

Table 1
Mix design of mixtures

Matrix type	Cement (kg/m^3)	Silica fume (kg/m^3)	Fly ash (kg/m^3)	Quartz (kg/m^3)	Aggregate			Superplasticizer (kg/m^3)	Water (kg/m^3)	W/B (-)
					C.G (kg/m^3)	F.S (kg/m^3)				
					6-8mm	0-4mm	150-600 µm			
NSC	364[a]	-	-	-	979	812	-	-	200	0.55
MSC	350[b]	-	107	-	660	1073	-	-	205	0.45
HSC	480[b]	-	45	-	850	886	-	6	210	0.40
UHPM	710[b]	230	-	210	-	-	1020	30.7	127	0.11

[a] Portland-limestone cement CEM II 32,5R
[b] Portland cement CEM III 52.5 N

Table 2
The measured geometric properties of fibre hook

Fibre type	L_f (mm)	D_f (mm)	f_y (MPa)	l_1 (mm)	l_2 (mm)	α (°)	β (°)
3D 65/60 BG	60	0.90	1150	2.12	2.95	45.7	47.5

Table 3
Mechanical properties of steel fibres at ambient and elevated temperatures

Temperature (°C)	Yield strength (MPa)	Ultimate strength (MPa)	Elongation at failure (%)
20	986	1170	5.6
100	958	1155	4.9
200	885	1159	4.9
300	801	1131	3.6
400	780	1130	3.4
500	556	818	3.1
600	387	437	21.1
700	274	348	22.4
800	144	287	24.6

Abdallah, S., Fan, M., Cashell, K.A. Bond-slip behaviour of steel fibres embedded in concrete after exposure to elevated temperatures. Construction & Building Materials, 2017; 140: 542-551.
http://www.sciencedirect.com/science/article/pii/S0950061817303495

Table 4
Bond parameters of straight fibre derived from test results

Material	Property	20°C	100°C	200°C	300°C	400°C	500°C	600°C	700°C	800°C
NSC	P_{max} (N)	165	122	102	84	74	57	56	52	27
	$\sigma_{f,max}$ (MPa)	260	192	160	132	116	90	88	82	42
	τ_{av}(MPa)	1.9	1.4	1.2	0.9	0.8	0.7	0.6	0.6	0.3
	τ_{eq} (MPa)	1.1	1.0	1.0	0.9	0.8	0.6	0.5	0.4	0.4
	W_{total} (N mm)	1435	1363	1384	1040	979	721	605	527	466
MSC	P_{max} (N)	177	171	144	113	107	105	104	77	64
	$\sigma_{f,max}$ (MPa)	278	269	226	178	168	165	164	121	101
	τ_{av}(MPa)	2.1	2.0	1.7	1.4	1.3	1.2	1.2	0.9	0.7
	τ_{eq} (MPa)	1.2	1.1	1.3	1.0	1.3	1.0	0.8	0.6	0.4
	W_{total} (N mm)	1566	1436	1641	1389	1598	1302	1003	857	533
HSC	P_{max} (N)	266	238	236	227	210	200	168	138	57
	$\sigma_{f,max}$ (MPa)	418	374	371	357	330	315	264	217	90
	τ_{av}(MPa)	3.1	2.8	2.7	2.6	2.4	2.3	1.9	1.6	0.6
	τ_{eq} (MPa)	1.8	1.5	1.8	1.4	1.3	1.2	1.1	0.4	0.3
	W_{total} (N mm)	2263	1932	2271	1871	1815	1558	1442	417	466
UHPM	P_{max} (N)	299	222	218	174	141	-	-	-	-
	$\sigma_{f,max}$ (MPa)	456	349	342	274	222	-	-	-	-
	τ_{av}(MPa)	3.4	2.6	2.5	2.1	1.6	-	-	-	-
	τ_{eq} (MPa)	1.9	1.6	1.1	1	0.5	-	-	-	-
	W_{total} (N mm)	2468	1993	1493	1338	702	-	-	-	-

Abdallah, S., Fan, M., Cashell, K.A. Bond-slip behaviour of steel fibres embedded in concrete after exposure to elevated temperatures. Construction & Building Materials, 2017; 140: 542-551.
http://www.sciencedirect.com/science/article/pii/S0950061817303495

Table 5

Bond parameters of hooked-end fibre derived from test results

Material	Property	20°C	100°C	200°C	300°C	400°C	500°C	600°C	700°C	800°C
NSC	P_{max} (N)	325	304	352	345	309	310	234	217	148
	$\sigma_{f,max}$ (MPa)	511	478	554	543	486	487	368	341	233
	τ_{av}(MPa)	3.8	3.5	4.1	4.1	3.6	3.5	2.7	2.5	1.7
	τ_{eq} (MPa)	2.0	1.8	2.3	2.1	2.2	1.6	1.4	1.3	0.9
	W_{total} (N mm)	2515	2280	2941	2635	2715	2035	1826	1751	1240
MSC	P_{max} (N)	414	438	463	446	376	269	259	182	151
	$\sigma_{f,max}$ (MPa)	651	689	728	701	591	423	407	286	237
	τ_{av}(MPa)	4.8	5.1	5.4	5.2	4.4	3.1	3.1	2.1	1.8
	τ_{eq} (MPa)	2.7	3.3	3.2	3.7	2.2	1.7	1.6	1.2	1.3
	W_{total} (N mm)	3542	4219	4137	4822	2861	2238	2098	1631	1690
HSC	P_{max} (N)	591	589	527	501	442	391	369	335	261
	$\sigma_{f,max}$ (MPa)	930	926	829	788	695	615	580	527	410
	τ_{av}(MPa)	6.9	6.9	6.2	5.9	5.2	4.6	4.3	3.9	3.1
	τ_{eq} (MPa)	5.3	3.7	4.4	4.1	3.3	3.1	2.9	2.6	2.5
	W_{total} (N mm)	6832	4759	5677	5309	4295	3916	3736	3359	3258
UHPM	P_{max} (N)	545	633	577	678	562	-	-	-	-
	$\sigma_{f,max}$ (MPa)	857	996	908	1066	884	-	-	-	-
	τ_{av}(MPa)	6.4	7.4	6.8	7.9	6.6	-	-	-	-
	τ_{eq} (MPa)	4.1	4.5	4.3	3.8	5.2	-	-	-	-
	W_{total} (N mm)	5248	5740	5489	4954	6656	-	-	-	-

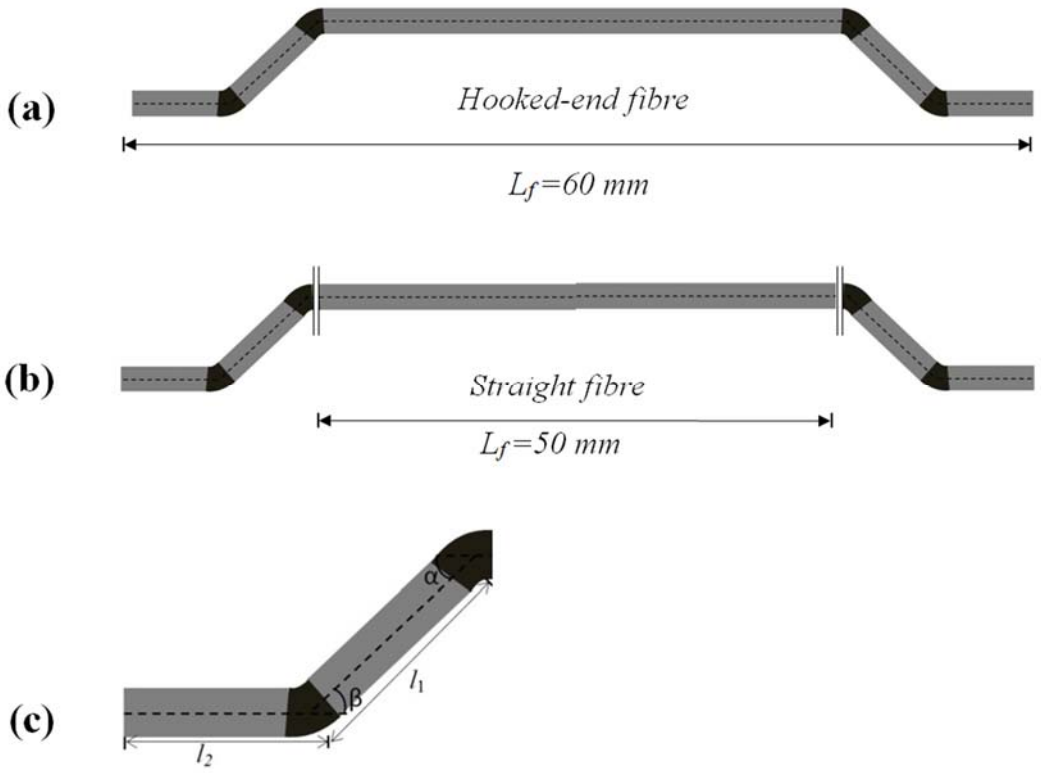

Fig. 1. Geometrical properties of (a) the hooked-end fibres, (b) straight fibres and (c) dimension of hook.

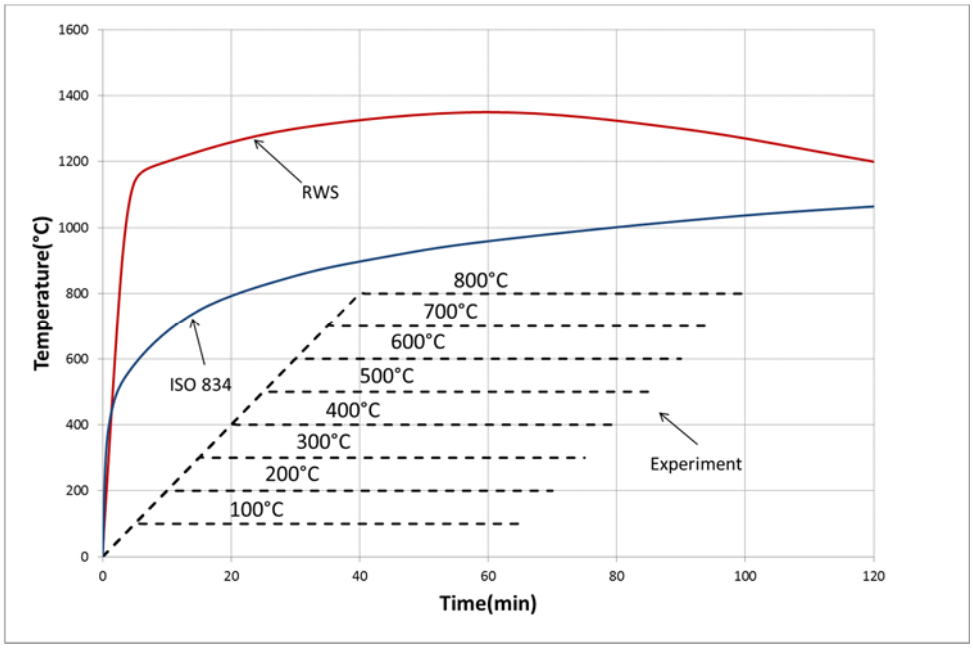

Fig. 2. Experimental heating rate compared with standard recommended temperature-time curves from ISO 834 [26] and RWS [27].

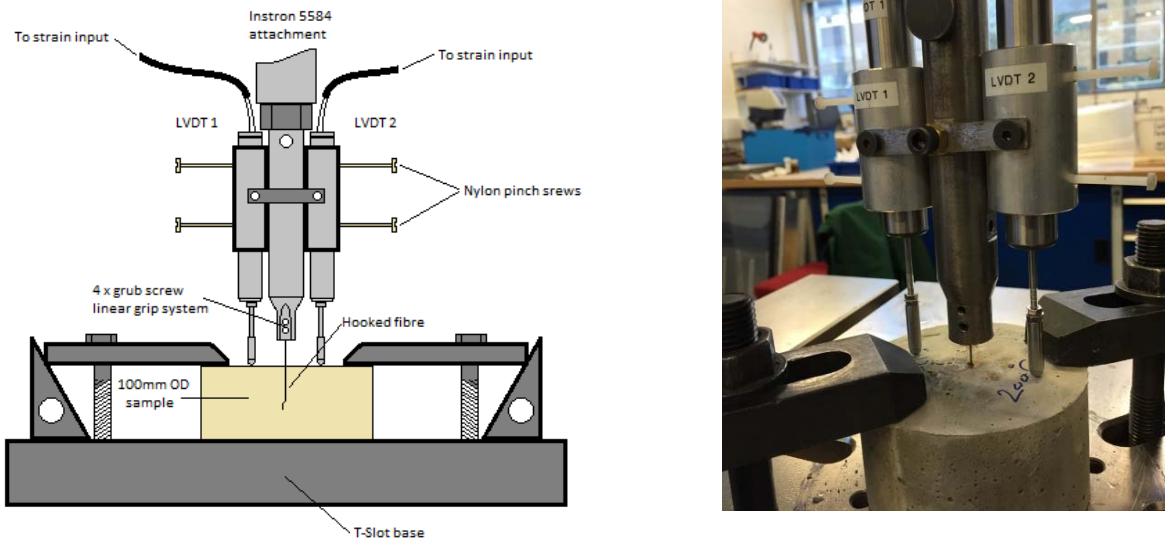

(a) (b)

Fig. 3. Set-up for pull-out tests: (a) schematic view and (b) photographic image during testing.

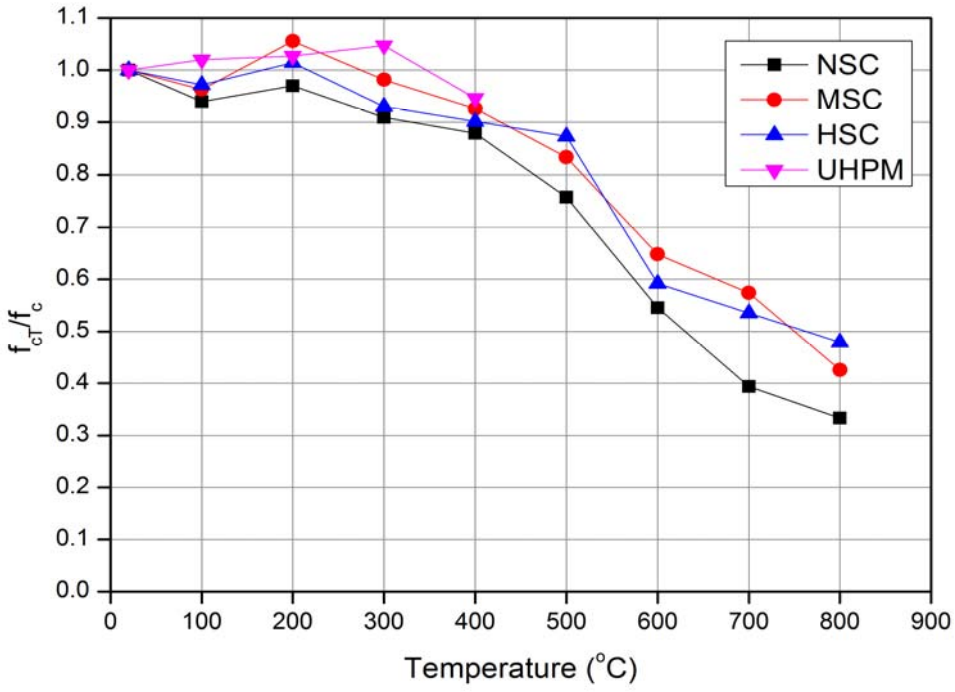

Fig. 4. Effect of elevated temperature on the compressive strength of concrete.

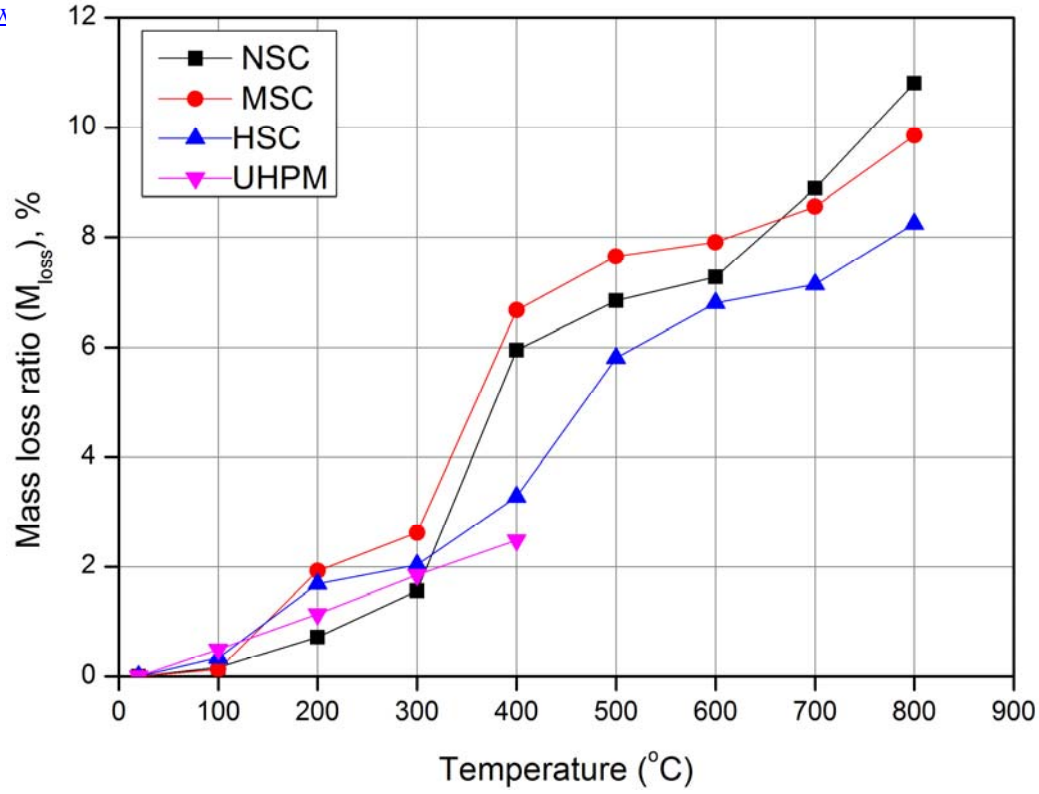

Fig. 5. Relationship between elevated temperature and mass loss.

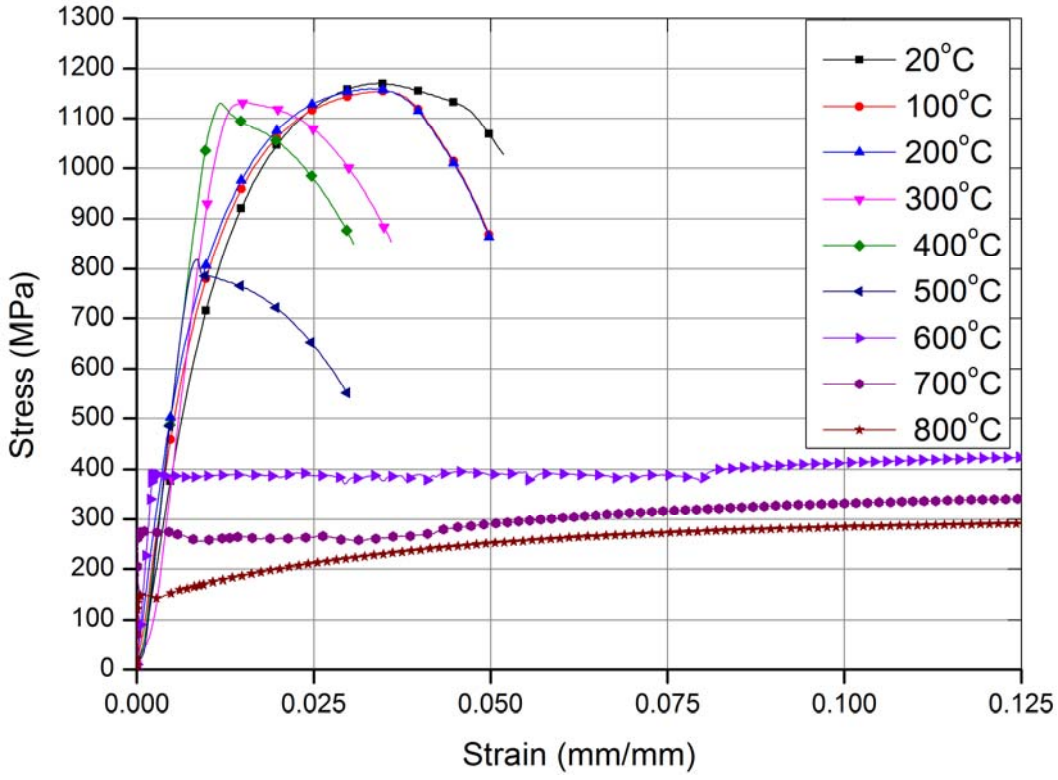

Fig. 6. Stress-strain curve for steel fibres at ambient and elevated temperatures.

Abdallah, S., Fan, M., Cashell, K.A. Bond-slip behaviour of steel fibres embedded in concrete after exposure to elevated temperatures. Construction & Building Materials, 2017; 140: 542-551.
http://www.sciencedirect.com/science/article/pii/S0950061817303495

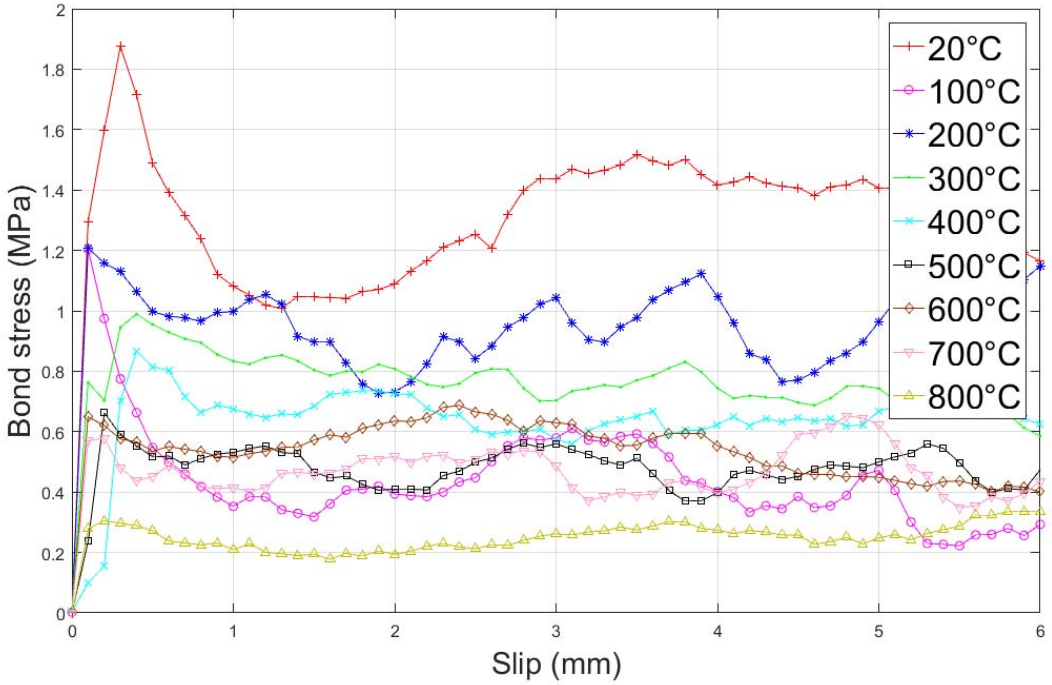

(a)

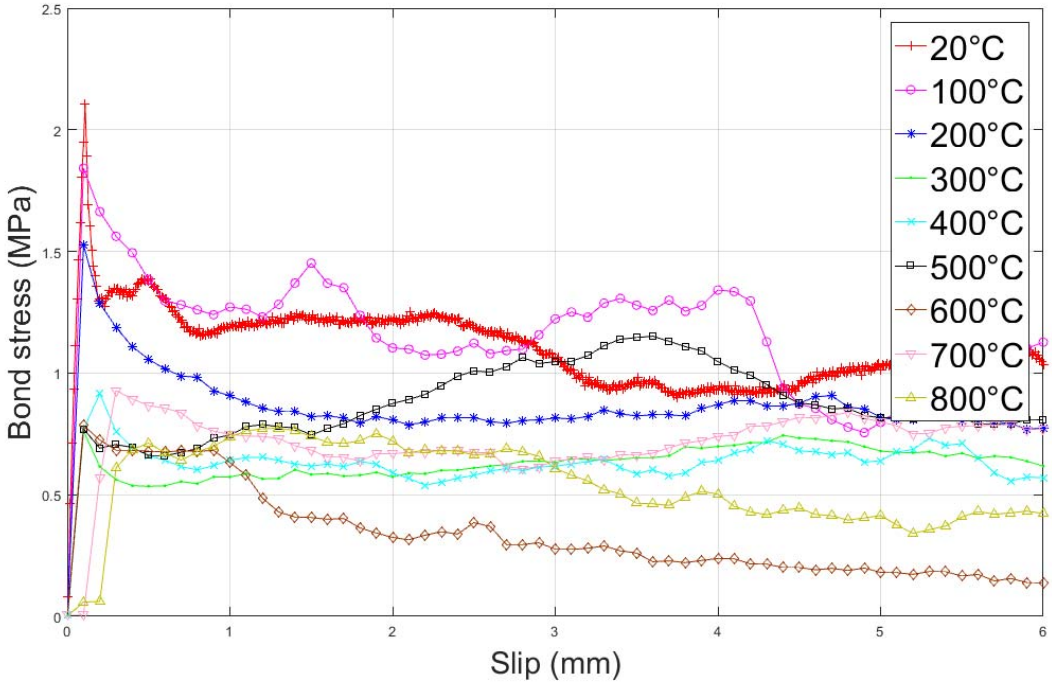

(b)

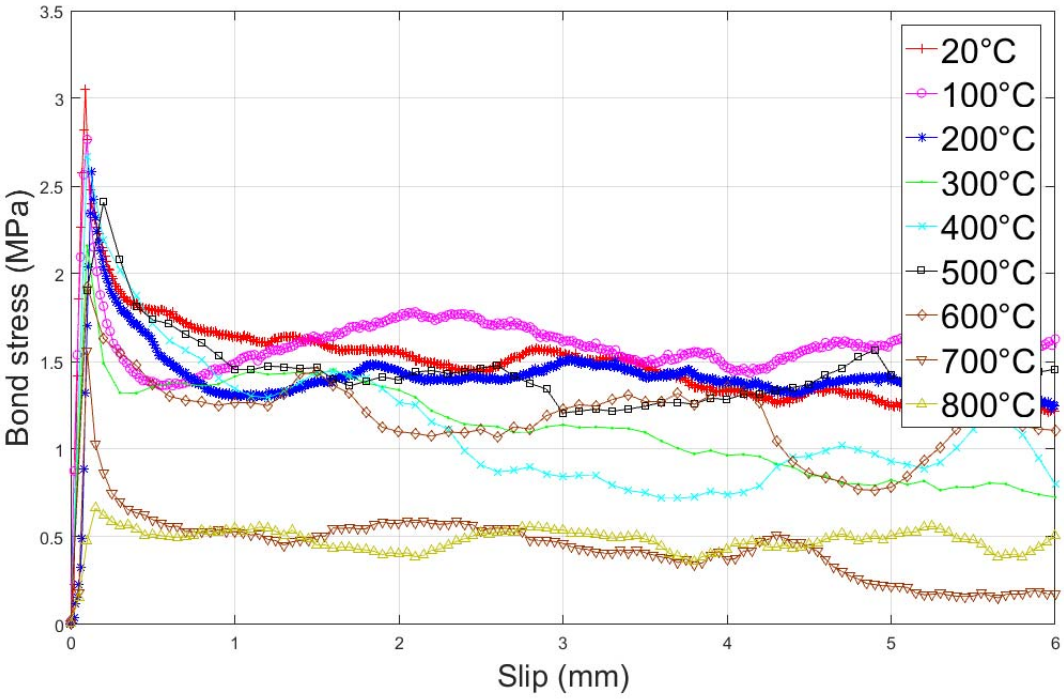

(c)

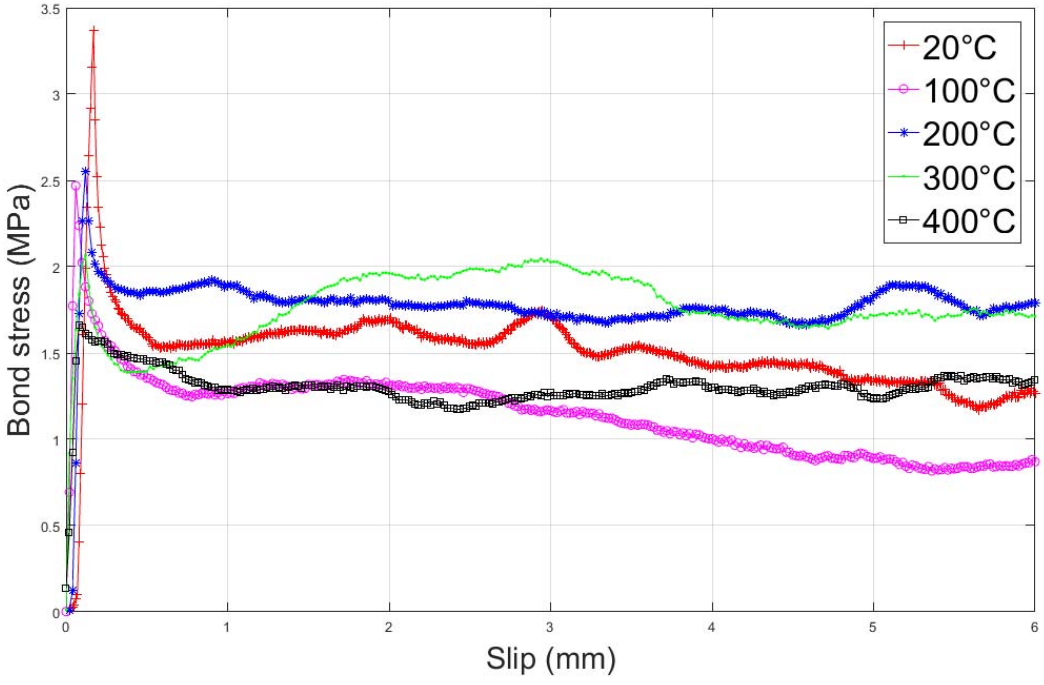

(d)

Fig. 7. Bond stress-slip curves of straight fibres embedded in (a) NSC, (b) MSC, (c) HSC and (d) UHPM.

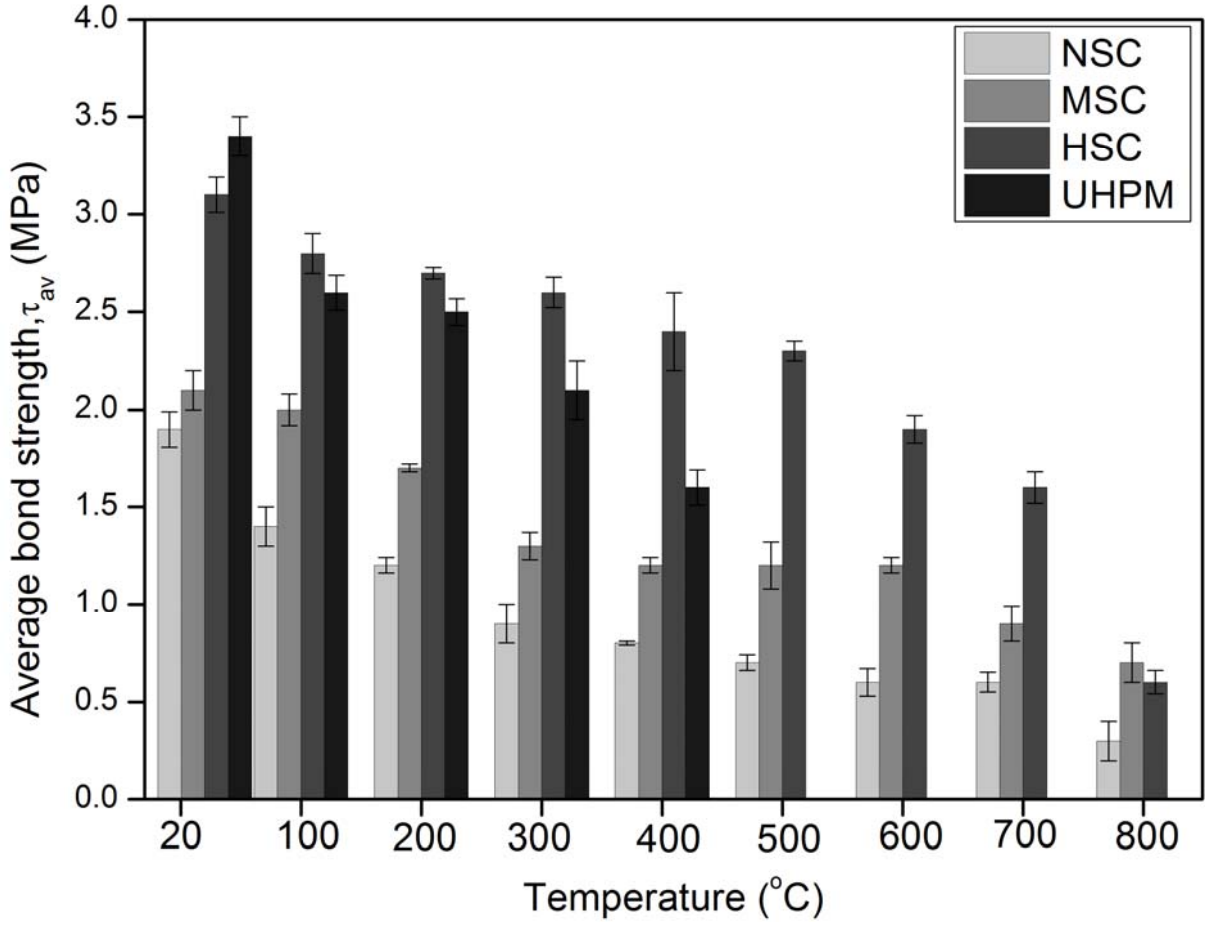

Fig. 8. Effect of elevated temperatures on the average bond strength of straight fibres

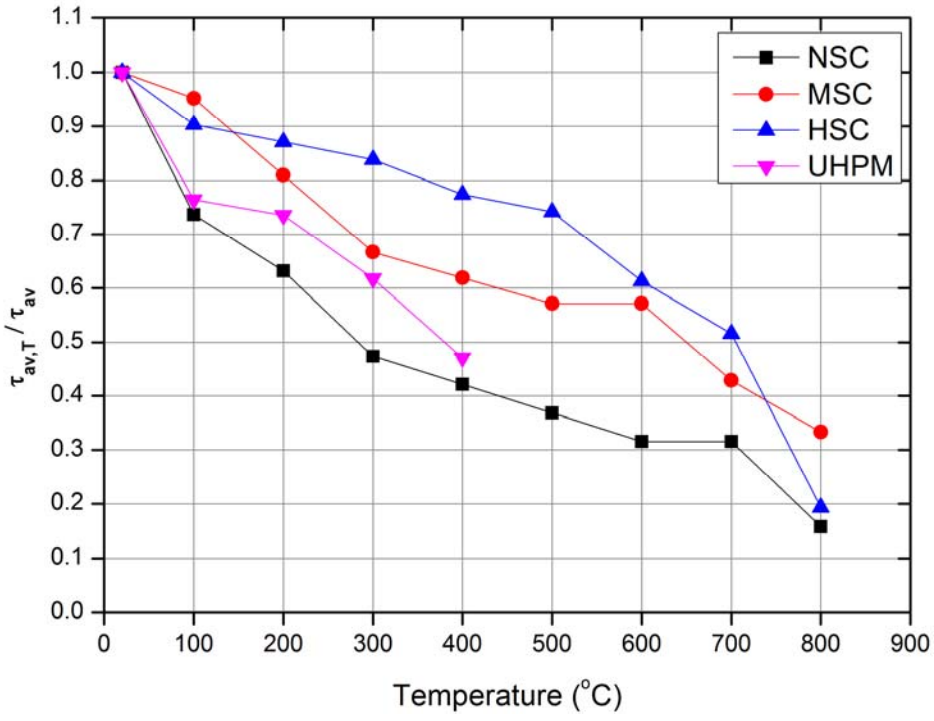

Fig. 9. Variation in the normalised average bond strength ($\tau_{av,T}/\tau_{av}$) of straight fibres embedded in NSC, MSC, HSC and UHPM as function of temperature

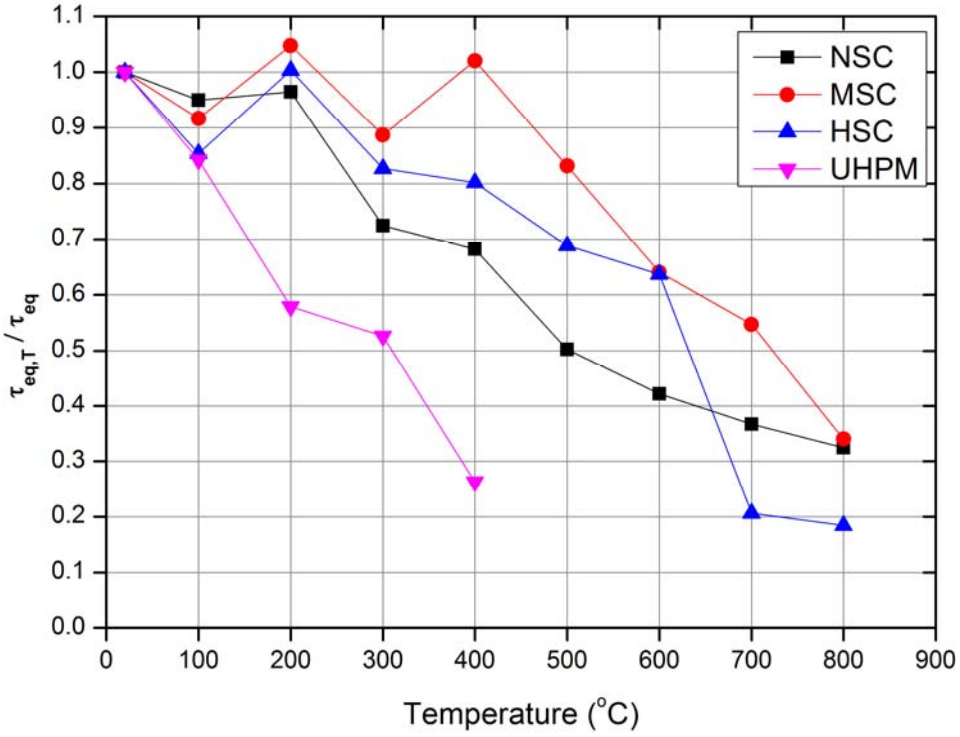

Fig. 10. Variation in the normalised equivalent bond strength ($\tau_{eq,T}/\tau_{eq}$) of straight fibres embedded in NSC, MSC, HSC and UHPM as a function of temperature

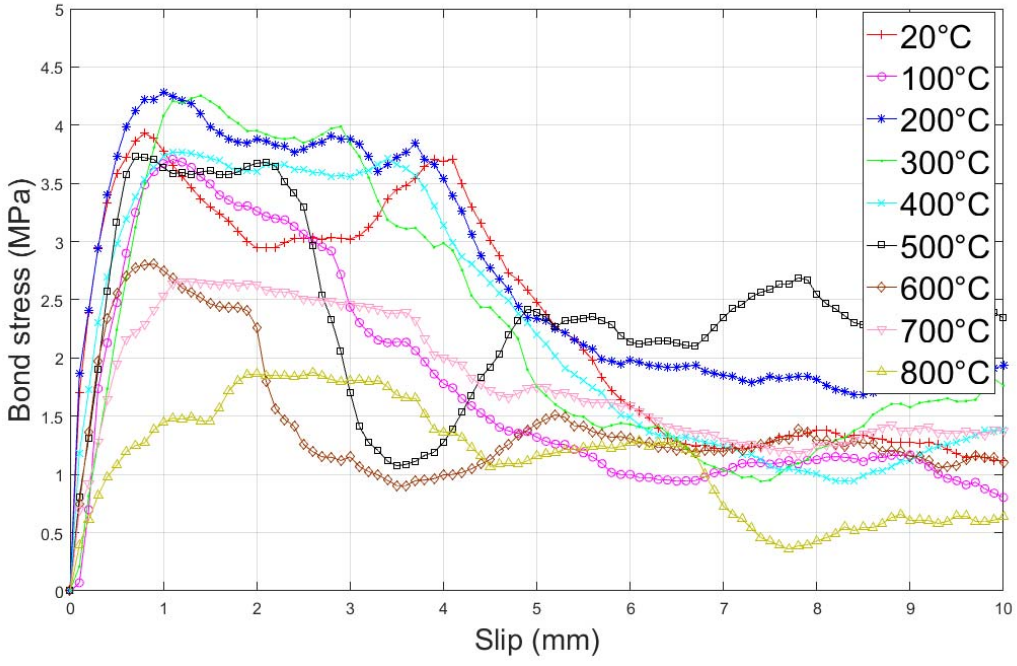

(a)

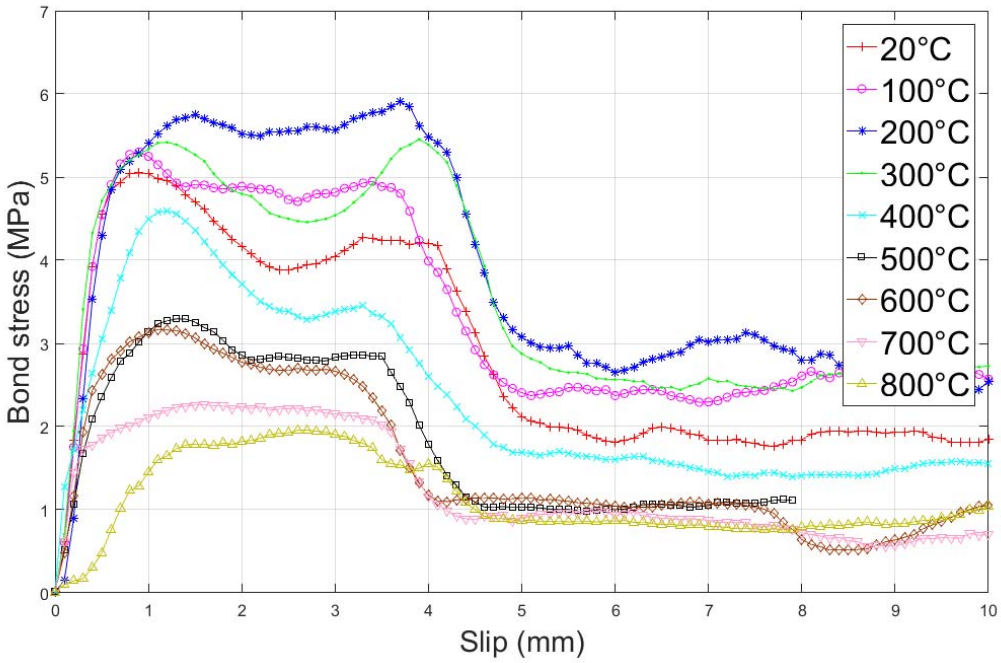
Bond stress (MPa)
Slip (mm)
20°C
100°C
200°C
300°C
400°C
500°C
600°C
700°C
800°C

(b)

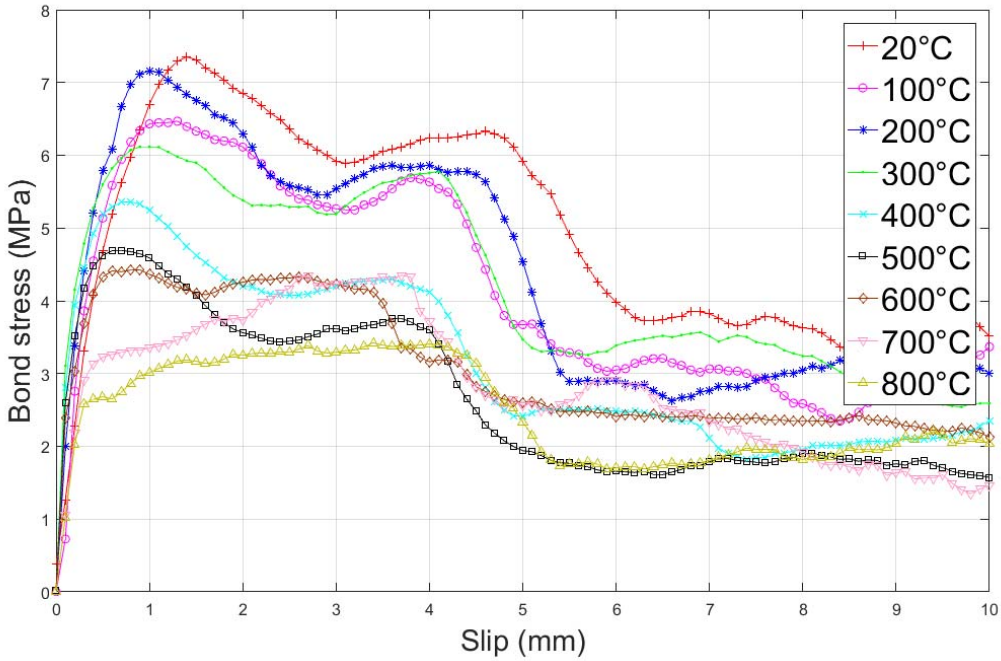
Bond stress (MPa)
Slip (mm)
20°C
100°C
200°C
300°C
400°C
500°C
600°C
700°C
800°C

(c)

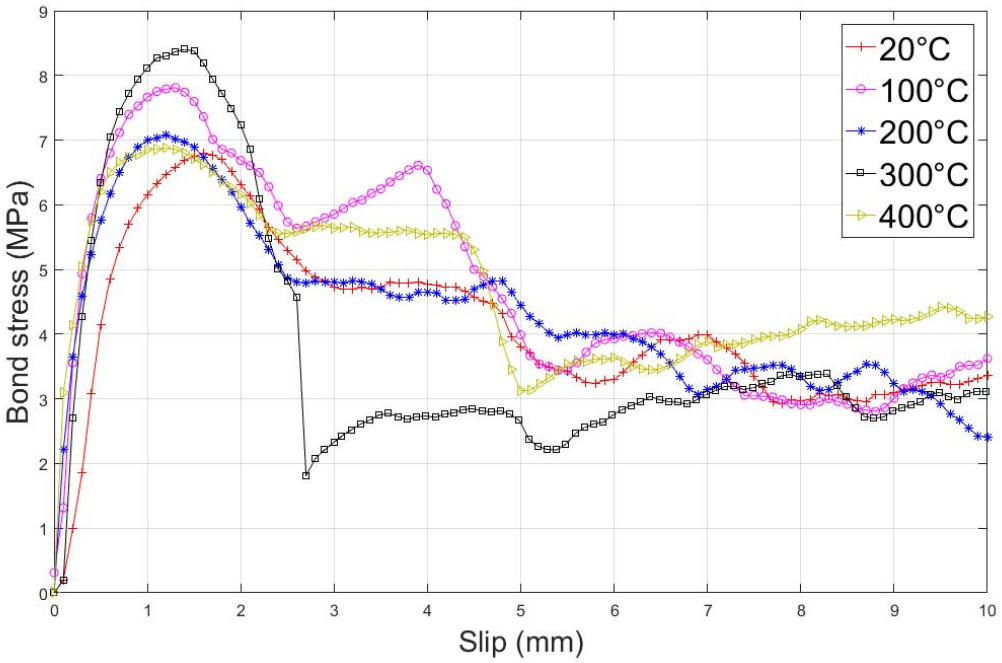

(d)

Fig. 11. Bond stress-slip curves of hooked-end fibre embedded in (a) NSC, (b) MSC, (c) HSC and (d) UHPM matrixes.

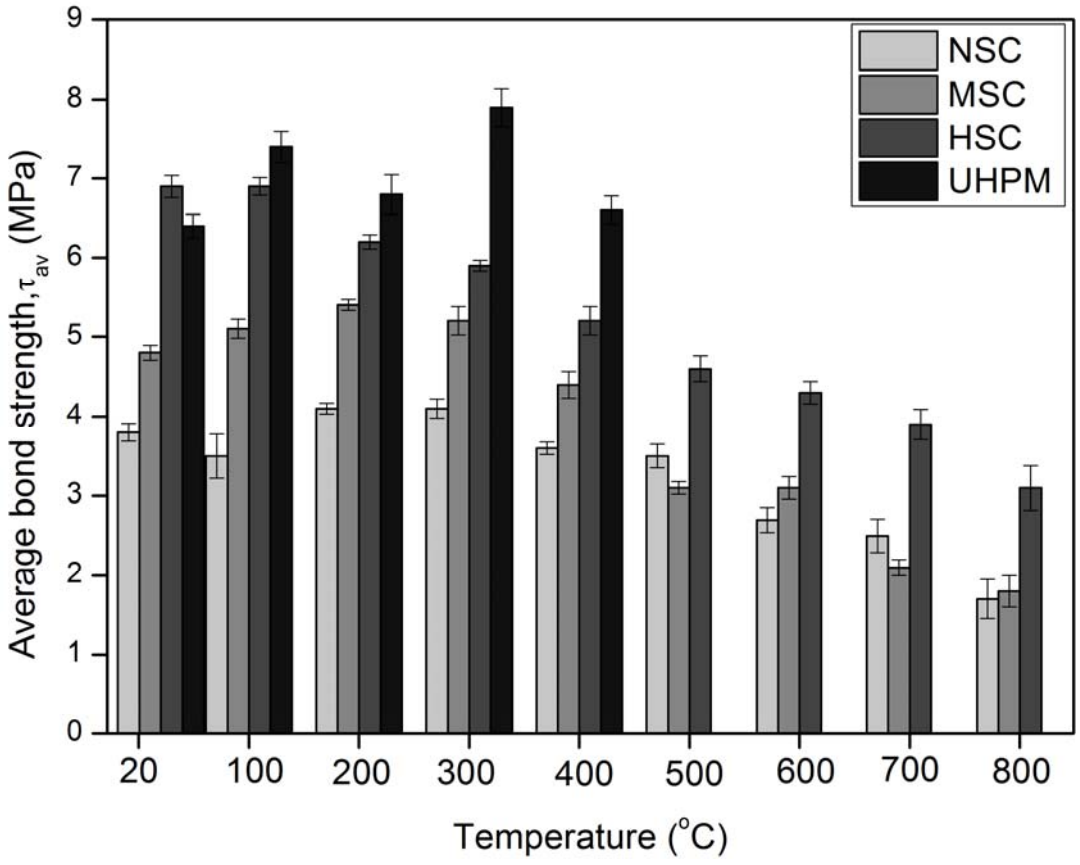

Fig. 12. Effect of elevated temperature on the average bond strength of hooked-end fibres.

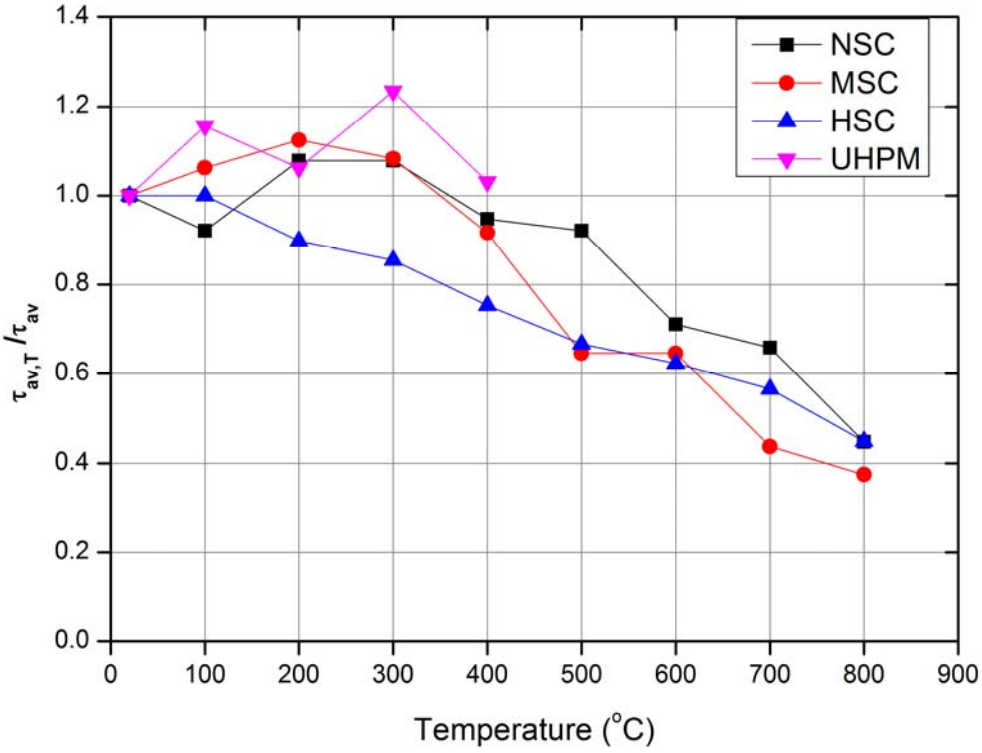

Fig. 13. Variation in the normalised average bond strength ($\tau_{av,T}/\tau_{av}$) of hooked-end steel fibres embedded in NSC, MSC, HSC and UHPM as a function of temperature.

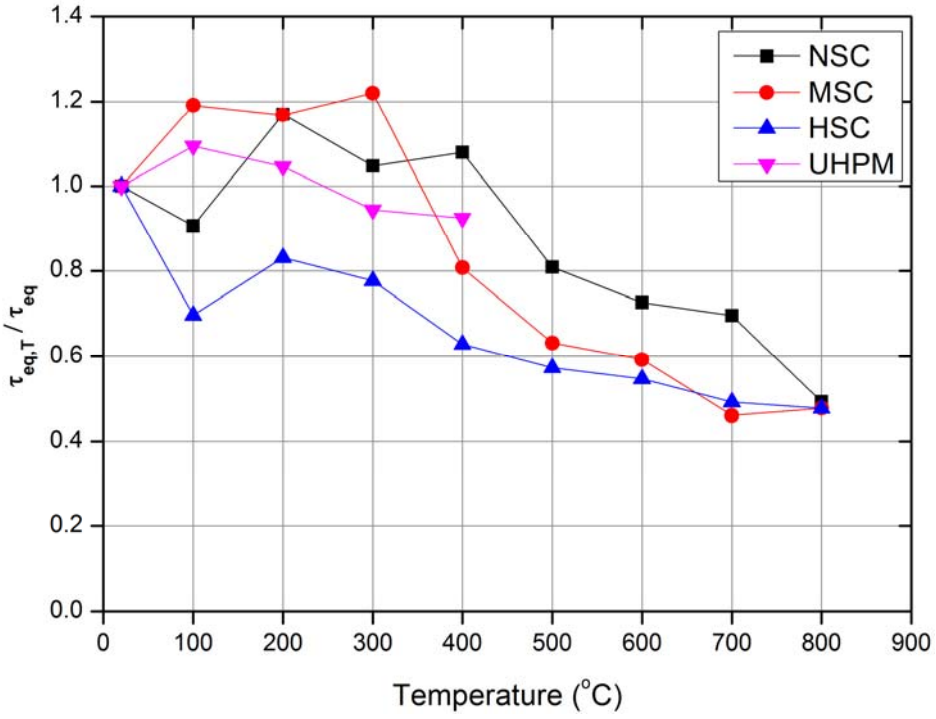

Fig. 14. Variation in the normalised equivalent bond strength ($\tau_{eq,T}/\tau_{eq}$) of hooked-end steel fibres embedded in NSC, MSC, HSC and UHPM as a function of temperature.

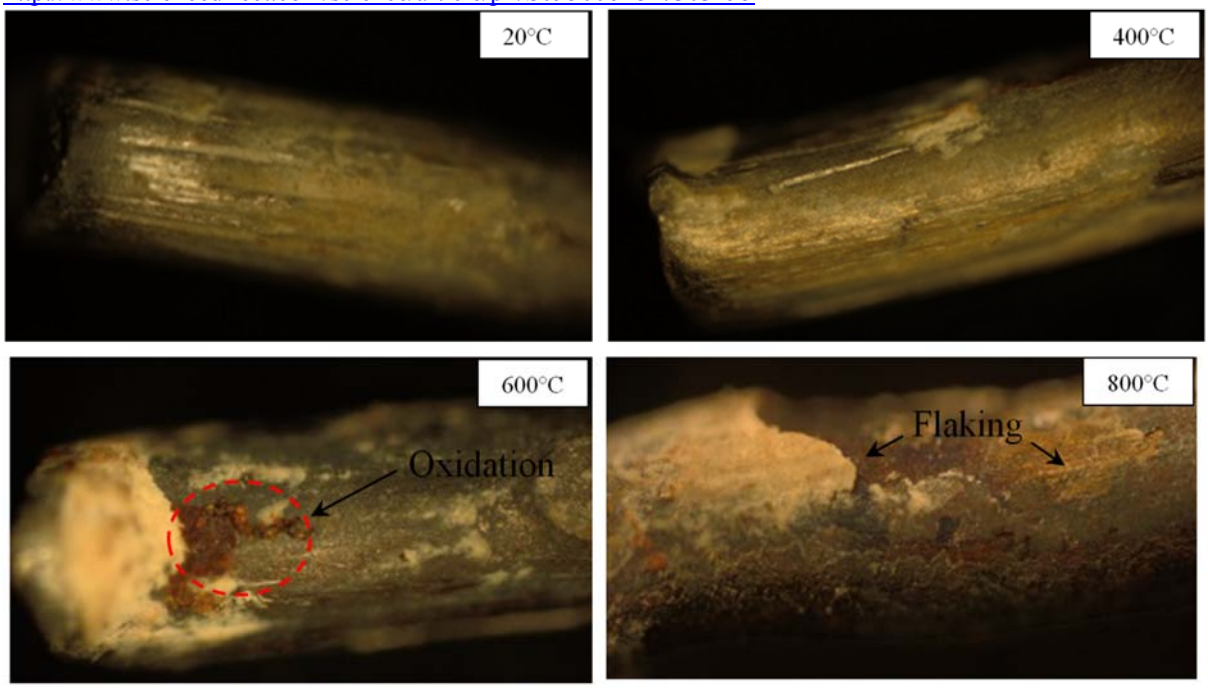

Fig. 15. Images of the damaged fibres which were embedded in normal strength concrete (NSC) following heating, cooling and pull-out testing